ISTITUTO NAZIONALE DI FISICA NUCLEARE

Sezione di Genova

INFN/AE–96/18
17 Giugno 1996

A. Buzzo, P. Musico, M. Pallavicini, C. Patrignani, E. Robutti:

A SILICON PAD DETECTOR FOR E–835 EXPERIMENT AT FERMILAB

SIS–Pubblicazioni
dei Laboratori Nazionali di Frascati

INFN – Istituto Nazionale di Fisica Nucelare
Sezione di Genova

INFN/AE–96/18
17 Giugno 1996

A SILICON PAD DETECTOR FOR E–835 EXPERIMENT AT FERMILAB

A. Buzzo[a)], P. Musico[a)], M. Pallavicini[b)], C. Patrignani[b)], E. Robutti[b)]

a) INFN – Sezione di Genova, Via Dodecaneso 33, I–16146 Genova, Italy
b) INFN – Sezione di Genova e Università di Genova, Via Dodecaneso 33, I–16146 Genova, Italy, Italy

Abstract

We have built a Silicon Pad Detector for experiment E-835 at the Fermilab Antiproton Accumulator to perform charmonium spectroscopy in the $\Phi\Phi \rightarrow 4K$ channel. It's a very compact cylindrical structure, with 4608 diodes (size 2.9×25.9 mm^2) arranged on 24 printed boards where two staggered layers of crystals and front end electronics are set. The detector is devoted to measure the z-coordinate (position along antiproton beam axis) with an accuracy better than 0.8 mm at a radius around 9 cm from the beam axis and with a full geometrical acceptance between 15 and 65 degrees in the polar angle and 360 degrees in azimuth. By putting two layers of crystals on each PCB and front-end electronics on the other face we could keep the total thickness of the detector below 3.5% X_0. Fast multiplexed read-out (5 MHz) allows to read the whole number of channels within 3.2 μs in order to handle the E-835 instantaneous luminosity of 3.0 $10^{31} cm^{-2} s^{-1}$ with a trigger rate around 5 KHz.

1 Introduction

The E-835 *Silicon Pad Detector* (SPD) will be installed at the Fermilab Antiproton Accumulator in spring 1996. Experiment E-835 [1] is devoted to the study of all charmonium states formed through $p\bar{p}$ annihilations obtained intersecting a cooled antiproton beam with an internal hydrogen gas jet target: this technique, extensively described elsewhere ([1,2]), provides a more powerful tool to search for new charmonium states and to measure their mass and width than those based on e^+e^- annihilations because all states can be directly formed and studied via their electromagnetic decay channels their resonance parameters depending only on $\bar{p}$ beam momentum resolution.

To study the pseudoscalar states ($J^{PC} = 0^{-+}$) in E-760 the only available electromagnetic channel was the two photon one, which is affected by a large background coming from $\pi^0\pi^0$ and $\pi^0\gamma$ channels ([5]); in order to improve our experimental sensitivity on these states we are going to study them using the $\phi\phi$ channels as well, namely:

$$p\bar{p} \rightarrow \eta_c, \eta_c' \rightarrow \Phi\Phi \rightarrow K^+K^-K^+K^- \tag{1}$$

$$p\bar{p} \rightarrow^1 P_1 \rightarrow \eta_c\gamma \rightarrow \Phi\Phi\gamma \rightarrow \gamma K^+K^-K^+K^- \tag{2}$$

In order to handle the large particle flux (instantaneous luminosity will be higher than 3. $10^{31} cm^{-2}s^{-1}$ at the $^1P_1$ energy (3.526 MeV in $p\bar{p}$ c.o.m. frame) with an accepted rate around 5 MHz) and to achieve the desired spatial resolution of 2 $mrad$ in ϕ and 3 $mrad$ in θ (polar angle measured from the $\bar{p}$ direction which defines the z axis of our reference system) we decided to build a compact Silicon Pad Detector (SPD), using a cylindrical geometry with internal radius 7.5 cm and external 10.0 cm.

The double layer pad structure of the detector together with its large geometrical acceptance (from 15 to 65 degrees in θ, 360 degrees in ϕ) provides a powerful tool to disentangle the $\Phi\Phi$ candidates from the huge adronic background using multiplicity and topological cuts, both simple and CPU time saving, which will be implemented in the third level software trigger. In fact, the tower structure of the SPD provides a quick way to correlate θ and ϕ measurements coming from other detectors.

This paper is structured as follows: section 2 describes the crystals geometry and their physical main features; in section 3 the front-end printed board design and crystal packing are shown; the whole detector mechanical structure

[1] This is the new name of experiment E-760 which has already accomplished part of the physical program on charmonium states during 1990 and 1991 runs ([1–6])

References

[1] T.A. Armstrong et al., *Study of the χ_1 and χ_2 charmonium states formed in $\bar{p}p$ annihilations.* Nucl. Phys., **B373**(1992)35.

[2] T.A. Armstrong et al., *Measurement of the J/ψ and ψ' Resonance Parameters in $p\bar{p}$ Annihilations.* Phys. Rev. **D47**(1993)772.

[3] T.A. Armstrong at al., *Observation of the $^1P_1$ state of Charmonium.* Phys. Rev. Lett. **69**(1992)2337.

[4] T.A. Armstrong et al., *Measurement of the Proton Electromagnetic Form Factors in the Time-like Region at* 8.9 *to* 13.0 *GeV^2.* Phys. Rev. Lett. **70**(1993)1212.

[5] T.A. Armstrong et. al., *Study of the η_c (S wave singlet) state of charmonium formed in $\bar{p}p$ annihilations and a search for the η_c' .* Phys. Rev. **D52**(1995)4839.

[6] T.A. Armstrong et. al., *Study of the angular distribution of the reaction $\bar{p}p \to \chi_2 \to J/\psi\gamma \to e^+e^-\gamma$* Phys. Rev. **D48**(1993) 3037.

[7] M. Pallavicini, *Tesi di Dottorato di Ricerca in Fisica (Ph.D Thesis)* Genova University.

[8] P. Musico et. al., *The E835 Silicon Pad Detector DAQ System* (to be submitted to **NIM A**)

[9] L. Evensen et. al., *Guard ring design for high voltage operation of Silicon Detectors* Nucl. Instr. & Meth. **A 337** (1993) 44.

[10] L. Evensen et. al., *A fast low noise silicon detector for electron spectroscopy up to 1 MeV* Nucl. Instr. & Meth. **A 326** (1993) 136.

[11] P. Jarron et. al., *AMPLEX, a low noise, low power, analog CMOS signal processor for multi element silicon particle detectors* Proc. 5th European Symposium on Semiconductor Detectors
Munich, Germany, February 1989.

Feature	Value	Unit
Length	25.60±0.05	mm
Width	26.00±0.05	mm
Thickness	350±20	μm
Pad dimension	2.85x23.9	mm
Pads separation	0.1	mm
Active area	561.65	mm^2
Pad per crystal	8	-
Guard ring width	950	μm

Fig. 1. *Silicon crystals geometry and main features*

and cooling system are reported in section 4 while cosmic rays and beam tests results are given in section 5.

2 Silicon crystals

Crystal [2] geometrical dimensions have been dictated by physical and practical considerations in order to obtain the desired accuracy in the measurement of the z-coordinate (around 0.7 mm using both layers) and to keep their cost at an affordable level [3] but many other considerations have been taken into account as well: a) the total surface to be covered (about 2000 cm^2 with two layers); b) the easiness in manipulating and mounting/dismounting the crystals on the PCB; c) the input capacitance of our amplifier (maximum 25 pF); d) the total cost.

All these requirements have led us to choose the geometrical dimensions shown in Table 1.

Each detector (see Figure 2) is $25.6 \times 26.0 \times 0.350$ mm^3 and is surrounded by a 0.950 mm wide guard ring which prevents bulk and surface currents to go into the DC coupled amplifier inputs.

This guard ring reduces the active area of each detector to 561.7 mm^2 (total area 665.6 mm^2) but improves its performance by dramatically reducing the

[2] Manufacturer: SINTEF,Postboks 124 Blindern,N-0314 Oslo,NORWAY

[3] Silicon processing is done on circular wafers whose diameter is (in our case) 101.6 mm; using rectangular crystals, geometry should be chosen to inscribe exactly a few of them in a circle in order to reduce scraps.

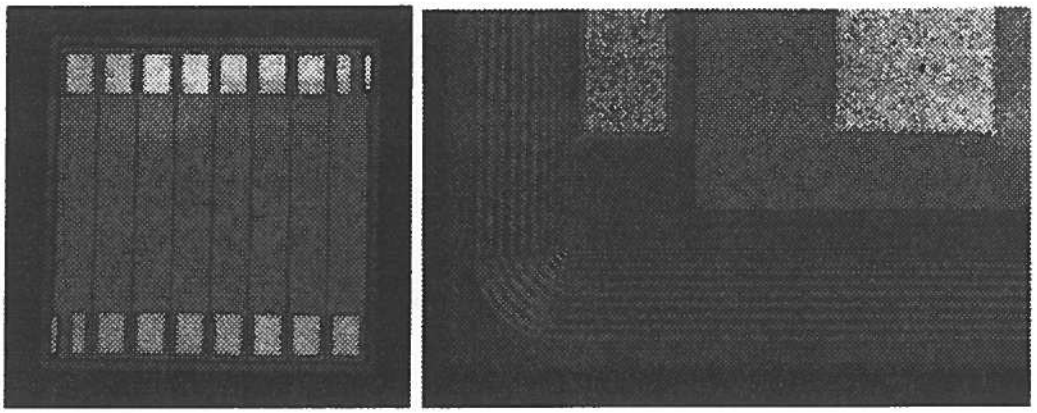

Fig. 2. *Left: Topview picture of a crystal; eight diode pads and one guard ring pad are clearly visible on both upper and lower side; the whole active area is surrounded by a nine-rings guard ring. Right: A detailed view of the guard ring.*

noise coming from leakage current fluctuations. Guard ring design is based on reference ([9]) and ([10]) and is optimized to keep pad currents around a few nA (maximum a few tens) even at temperature around 40-50 degrees Celsius.

To choose the appropriate thickness for the crystals we had to trade off between the experimental request to have very small thickness and our need to reduce diode capacitance at the amplifier inputs, thus achieving a good signal/noise ratio: with 350 μm detectors the total radiation length seen by a particle traversing the crystal at 90 degrees is around 0.4 % X_0, less than 20% of the total thickness and the input capacitance is around 25 pF, the maximum value allowed by our amplifier.

The back side of the crystal is covered with an aluminium layer (thickness 20 μm) which allows to supply a positive bias voltage to the diodes. This solution has been mostly dictated by the lack of space for the de-coupling capacitors we should have put in if we had used a negative bias on the pads. The estimated fluence of minimum ionizing particles crossing one cm^2 of the detector during the whole data taking is around 10^{12}, therefore we do not expect a big increase in pads currents due to radiation damage.

Depletion voltage, guard ring current and pad currents have been carefully measured for each detector in order to gather on the same PCB crystals with similar depletion voltage[4] on the same PCB and to identify and reject bad ones; results are shown in Figure 3.

[4] On each PCB (see section 3) 24 crystals are biased by the same line: crystals with very different depletion voltage would be either inefficient because of their incomplete depletion or noisy

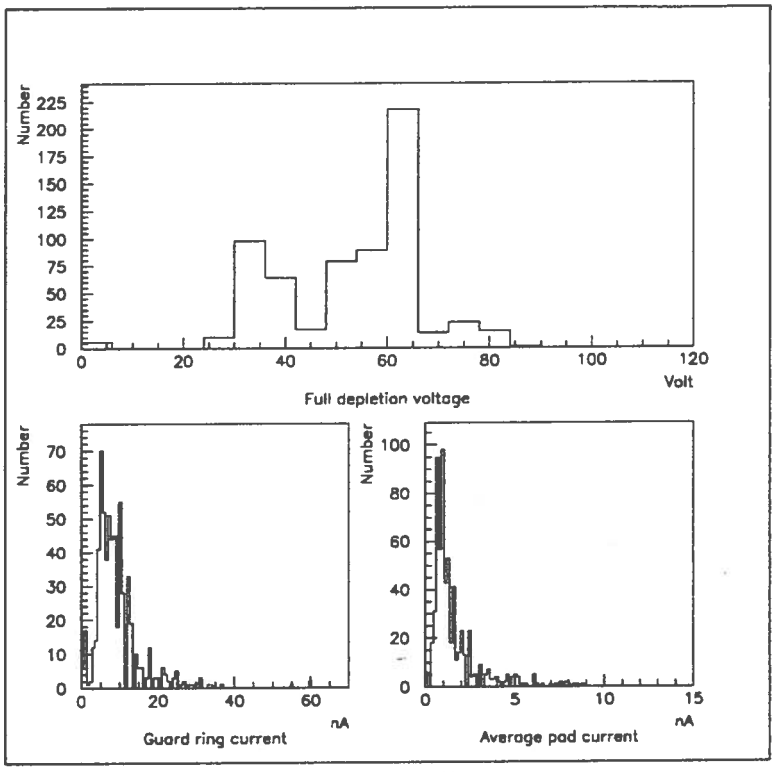

Fig. 3. *Crystal measurement results for the whole sample of 630 detectors. Upper plot is the full depletion voltage distribution, which shows a two peak structure, due to different doping concentration on silicon substrate. Lower plots are the guard-ring current distribution and the pad current distribution (average over 8 pads).*

We note, in particular, that the crystals are divided in two main groups, one with full depletion voltage around 30 V, the second around 60 V. This fact, due to different doping concentration on the n-type substrate, has no measurable effect on detection efficiency (see section 5).

3 Printed board

The Printed Circuit Board (PCB) is 1.0 *mm* thick, 34.0 *mm* wide and 380 *mm* long (or 390 *mm* [5]); it is built with three layers of vetronite 200 μm thick, each of them with two layers of copper for electrical connections.

[5] There are circuits of two different length to reduce interference between connectors in the downstream end of the detector but the active area and the geometry of the crystals mounted on them is exactly the same for both types

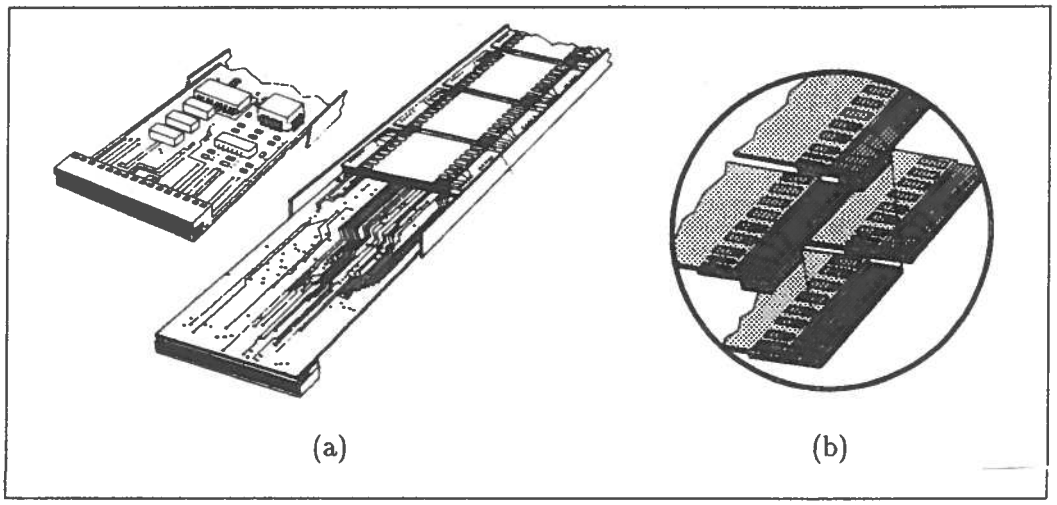

Fig. 4. *This pictures show the structure of one slab; (a) shows the two face of one PCB seen from the connector side; vetronite walls, electronic components and silicon crystal are shown as well; (b) shows a magnified view of the crystal side.*

Front-end electronics (on one side) and the double layer of silicon detectors (on the other side) are both set on the PCB, as shown in Figure 4 (a). Its weight, excluding electronic components and silicon detectors, is 33.5 g (short) and 35.0 g (long), corresponding to a 90 degrees radiation length of 0.8% X_0, mainly due to copper layers.

After soldering all electronics and connector the total weight reaches 54.5 g (short) and 56.0 g (long). The estimated averaged total radiation length (including silicon crystals) becomes 2.8% X_0, giving a ratio between active material thickness and total thickness around 1 : 3.5

To assure a sufficient rigidity to be able to support each PCB in the way shown in the next section, two vetronite walls (0.5 *mm* thick, 7 *mm* wide, 350 *mm* long) are glued to the PCB as shown in Figure 4 (a).

The following two sections give a brief description of the PCB structure and of the front-end electronics. A detailed one can be found in [7].

3.1 Silicon detectors layout

Silicon diode detectors are arranged on one side of the PCB in two layers of 12 crystals each staggered by 13 *mm* (half a crystal) along the z coordinate in order to eliminate inefficiencies due to the geometrical crack (0.3 *mm*) between two crystals; each detector is glued to two small vetronite circuits (0.5 *mm* $\times$ 5.5 *mm* $\times$ 26.0 mm) that are attached to the PCB via 10 golden tungsten wires (diameter 100 μm).

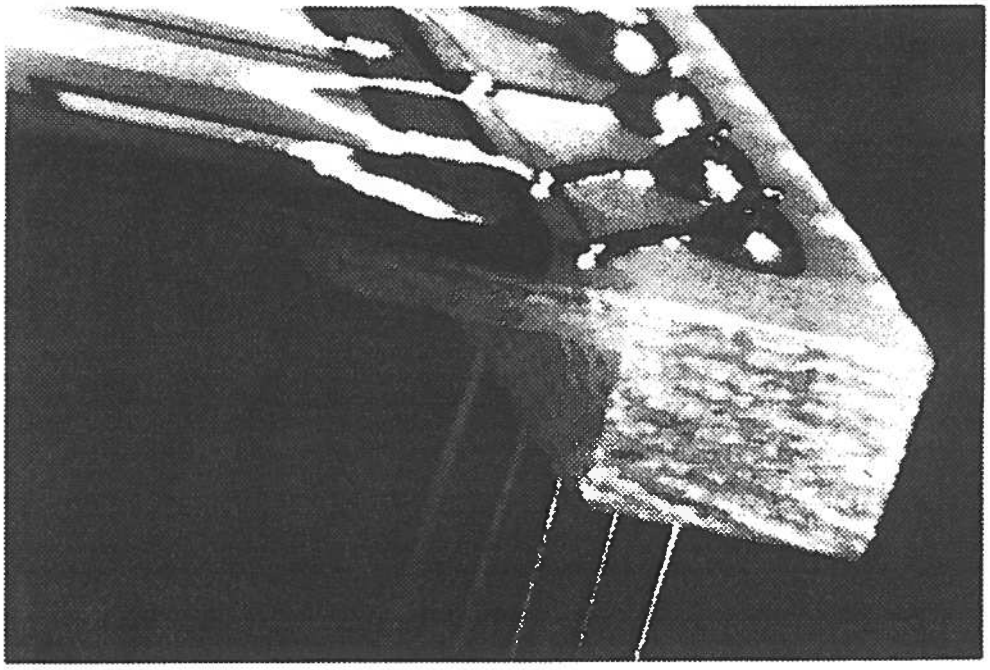

Fig. 5. *Three dimensional picture (magnification $\simeq$ 10) of a crystal glued and bonded on its vetronite circuit (upper layer, guard ring side): wire bondings, printed lines, solderings, tungsten wires and the 2 mm spacer are clearly visible.*

All diodes are connected to the vetronite supports using the wire-bonding technique, as shown in Figures 5 and 6. One of the two vetronite support has a small copper pad that is used to supply the polarization voltage to the diodes through a drop of conductive glue[6] while 10 tungsten wires carry the bias voltage, the guard ring connection to ground and the 8 diodes signals. As shown in Figure 4 (b), all wires pass through appropriate holes[7] (diameter 0.5 mm) and are soldered to the other side.

To reduce the inefficiencies due to bad connections, we chose to put two wire-bondings in each pad, using aluminium wires with diameter 20 μm; thence there are 18 bonding connection per crystal (for 8 diodes and the guard-ring), 432 each slab, 10368 for the whole detector.

The upper layer supports have a spacer 1.5 mm thick to keep crystals in the correct position and to avoid short cuts between the aluminium layer and lower layer's wire-bondings.

---

[6] We have used the conductive glue EPO-TEK H20E (resistivity $10^{-4}\Omega cm$) and the non-conductive one EPO-TEK 353ND

[7] Holes pitch in the vetronite supports has been chosen to be able to use the same production mask for both layers.

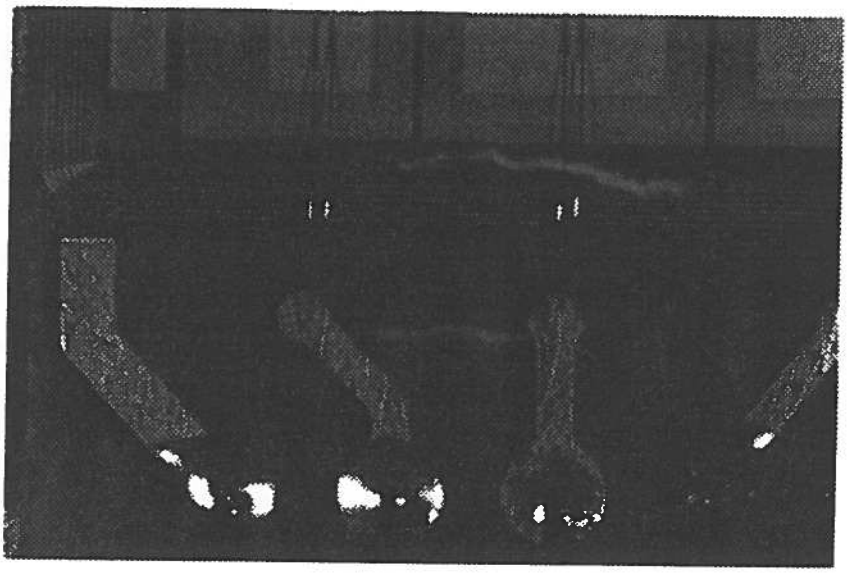

Fig. 6. *Top view picture (magnified 7 times) of a crystal glued and bonded on its vetronite circuit; the left line that goes under the crystal is connected to the alluminium face through a drop of conductive glue. Each pad is bonded twice to reduce inefficiencies due to bad connections. The lower spherical drops are the tungsteno wires solderings.*

3.2 Front-end electronics

24 crystals are arranged on each PCB, therefore 192 independent channels must be read. It has not been possible to read out the whole number of channels in parallel because of lack of space for the cables; furthermore we could not read out the whole PCB serially because the total read out time would have not fit the experiment requirements (total read-out time around 35 μs for a 50 long-words event).

We chose to compromize between these two issues by using a 16 channels chip amplifier with analog multiplexed read-out produced by SSS [8], named ICAR16 (see [11]). Each ICAR16 (see Table 8) can perform amplifying, shaping and track-and-hold of each input channel; the multiplexed analog read-out can be performed at a speed as high as 5 Mhz, giving a total read-out time of $3.2\mu s$.

12 ICAR16 chips are set on each PCB, to read out 192 channels. Figure 9 shows the block diagram of one read-out section: two silicon crystals (16 pads), one ICAR16 chip, one ECL comparator (Maxim MAX906), one DAC channel for the threshold (Analog Devices DAC-8800) and a buffer (Motorola MC34182) to drive the DAC output. The ICAR16 analog output signal is discriminated by an ECL-compatible voltage comparator. It should be noted that the comparator is triggered by a positive transition while ICAR16 by a

[8] Smart Silicon System S.A., Avenue de Chailly 23, CH-1012 Lausanne, Switzerland

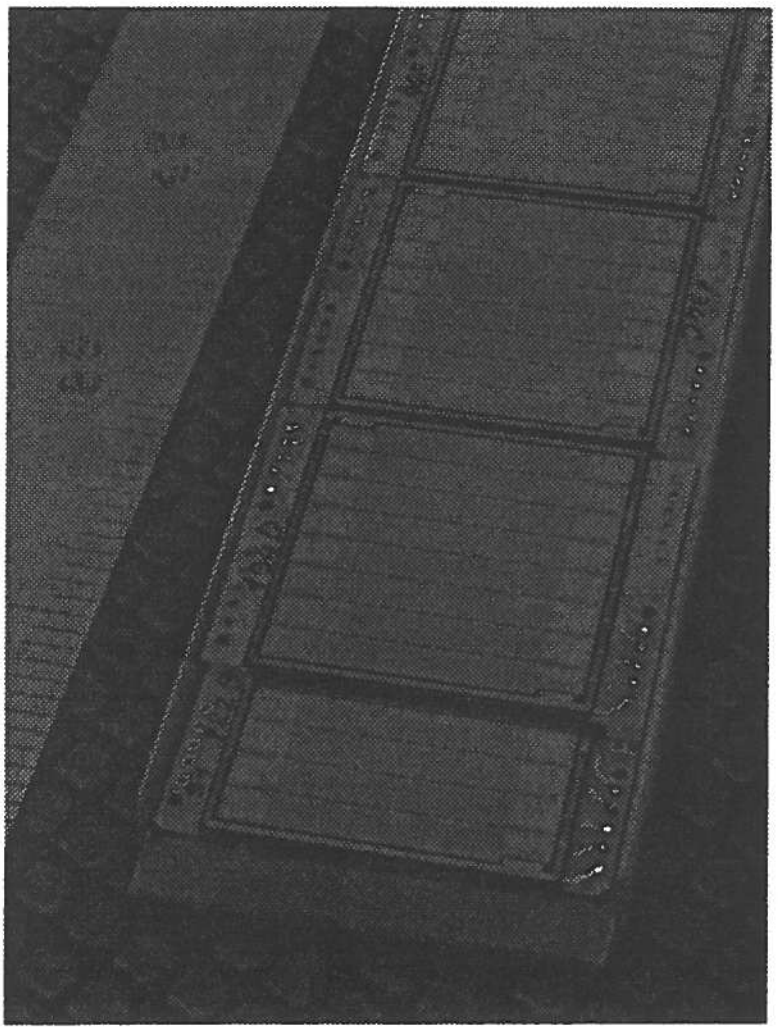

Fig. 7. *Magnified picture of the crystal side of a slab*

negative one, therefore the same signal can control both devices taking into account the time response of ICAR16 output stage. Furthermore MAX906 output impedence is low enough to drive the 5 m twisted-pair line needed to deliver its output signal to the VME read-out electronics, so no additional driver is required.

All ECL digital signals that control ICAR16 (Track & Hold level, Chip Select level and multiplexing 5 MHz Clock) are supplied from the external[9] electronics [8].

All detecting diodes are DC connected to the amplifier inputs; due to a mistake in final ICAR16 production, a few nA steady current must be put into amplifier inputs through a resistor.

Figure 10 shows the output waveform of an ICAR taken during a test beam

[9] Two MC10H116 triple line receivers are used to re-form all ECL signals

Parameters	Min	Typical	Max	Unit
Power				
V_{ref}	-2.25	-2.5	-3.25	V
V_{ss}	-4.5	-5.0	-5.5	V
Current absorption				
Ground	-	17	34	mA
V_{ss}	-	-10	-20	mA
V_{ref}	-	-7	-14	mA
Gain	32	40	48	mV/fC
Peaking time	150	200	320	ns
Input eq. noise	-	-	1000	e^-
Read out frequency	-	5	-	MHz

Fig. 8. *ICAR 16 main features*

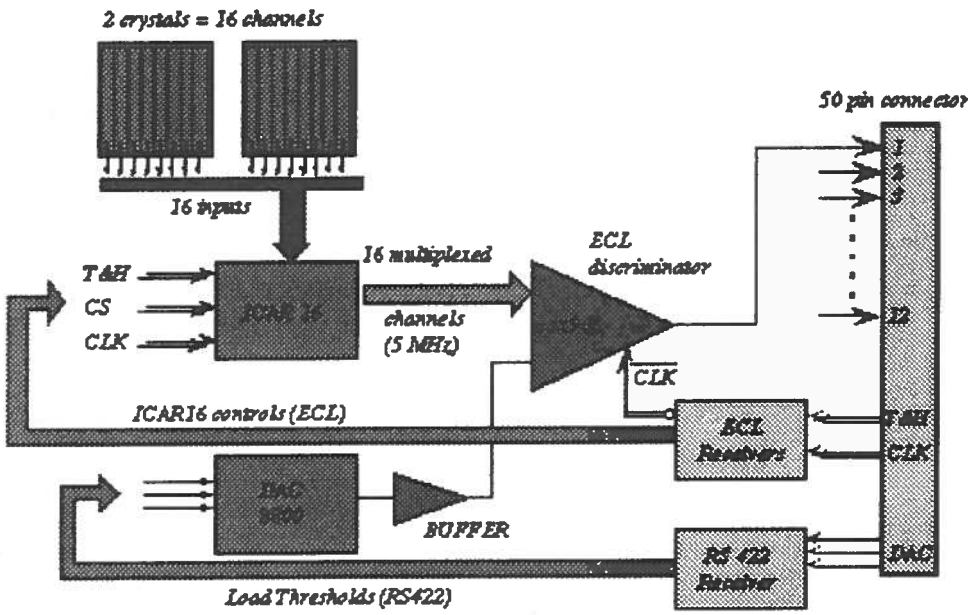

Fig. 9. *This picture shows a block diagram of one front-end electronics module; the main component ICAR 16 is shown together with two silicon crystals (16 channels), ECL discriminator and a DAC for the threshold (with a buffer); ECL receivers for ICAR16 control signals and RS422 receivers for thresholds loading are also shown.*

at CERN with a digital scope. The particle signal and the other 15 empty channels are clearly visible.

The 50-pin connector is set at one end of the PCB; all input and output signals are delivered through a flat cable plugged into this connector, except -5V power and ground because of the relatively high resistance of the wires [10].

The total power absorbed by one PCB is around 5 W (750 mA through -5V and 300 mA through +5V).

In order to be able to test both the front-end electronics and the connections of the diodes to the ICAR16 inputs, we have put on the PCB two different test lines named T1 and T2; the former allows to inject a charge signal on the diodes through the bias line; the latter takes the charge signal directly to the ICAR16 input through a small capacitor built into the PCB from two small copper pads. These two circuits have shown up to be very useful to debug the system and to find out bad components or connections.

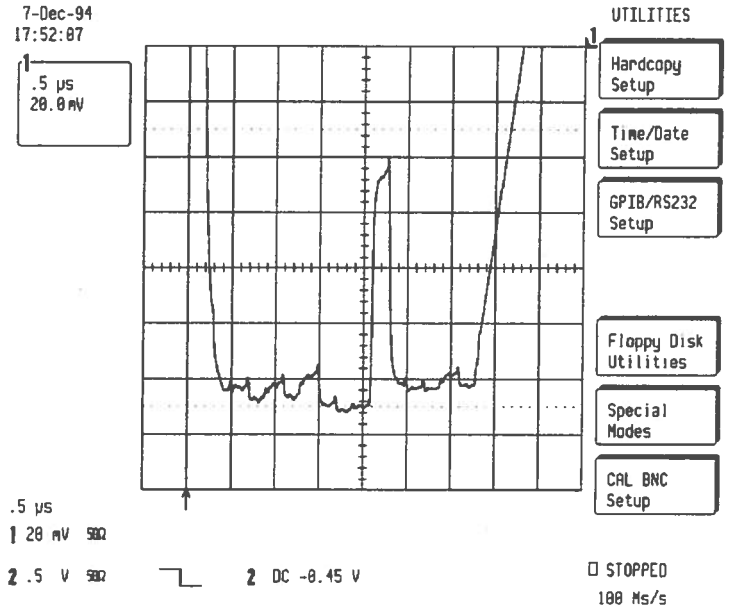

Fig. 10. *ICAR16 output waveform triggered by a real minimum ionizing particle; this picture has been taken with a digital scope (Le Croy ScopeStation 140) triggered by the coincidence of three scintillators aligned with the detector. The analog multiplexed signal is 3.2 µs, corresponding to 16 channels at 5 MHz. Pad 11 has been hit by a 5 GeV/c pion.*

[10] Flat cable pitch is 0.635 *mm* and single wire resistance is around 2 Ω giving a voltage drop on -5V power around 1.5 V that, of course, cannot be tolerated

4 Mechanical structure

As already said in section 1, we chose to build a cylindric shape detector in order to match the existing detector geometry. The structure is shown in Figure 11 together with part of the hydrogen jet target to which the detector is hung.

The 24 PCBs are arranged in a double layer barrel geometry with a carbon fiber cylinder and two vetronite flanges to support the whole structure (see Figure 12). The 12 short PCBs are mounted at a radius of 8.15 *cm* while long PCBs are set at radius 9.05 *cm*. The overlap in azimuth acceptance of the two layers is around 0.5 degrees to avoid inefficiencies due to misalignment. The support cylinder is 0.6 *mm* thick, has internal radius 75.5 *mm* and is 403 *mm* long.

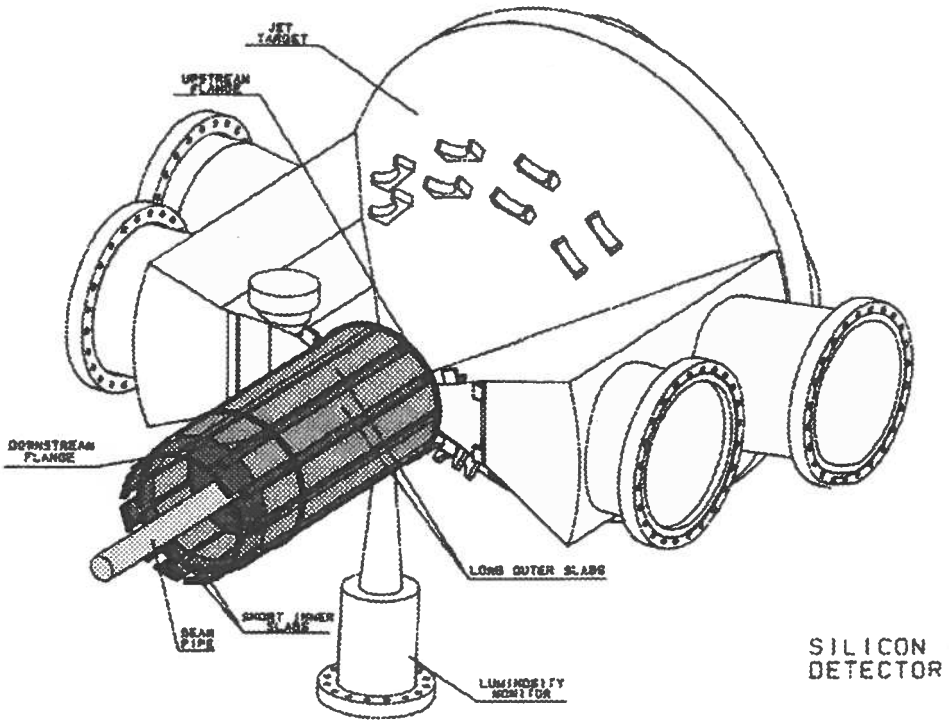

Fig. 11. *Picture view of the Silicon Pad Detector and part of the jet target to which the detector is hung; inner and outer slabs are clearly visible together with the inner support cylinder, the two vetronite flanges and part of the beam pipe; this picture does not show the outer vetronite sheet that covers the whole cylinder and flat cables that must be plugged to the downstream connectors.*

The first flange has been built from a single piece of 5 *mm* thick stesalite and can support the whole cylinder through 4 screws; also mounted on the flange are 6 gas inlets (8 *mm* diameter) to provide the cooling air flow. The second flange, built in stesalite as well, keeps the 24 circuits in the correct position.

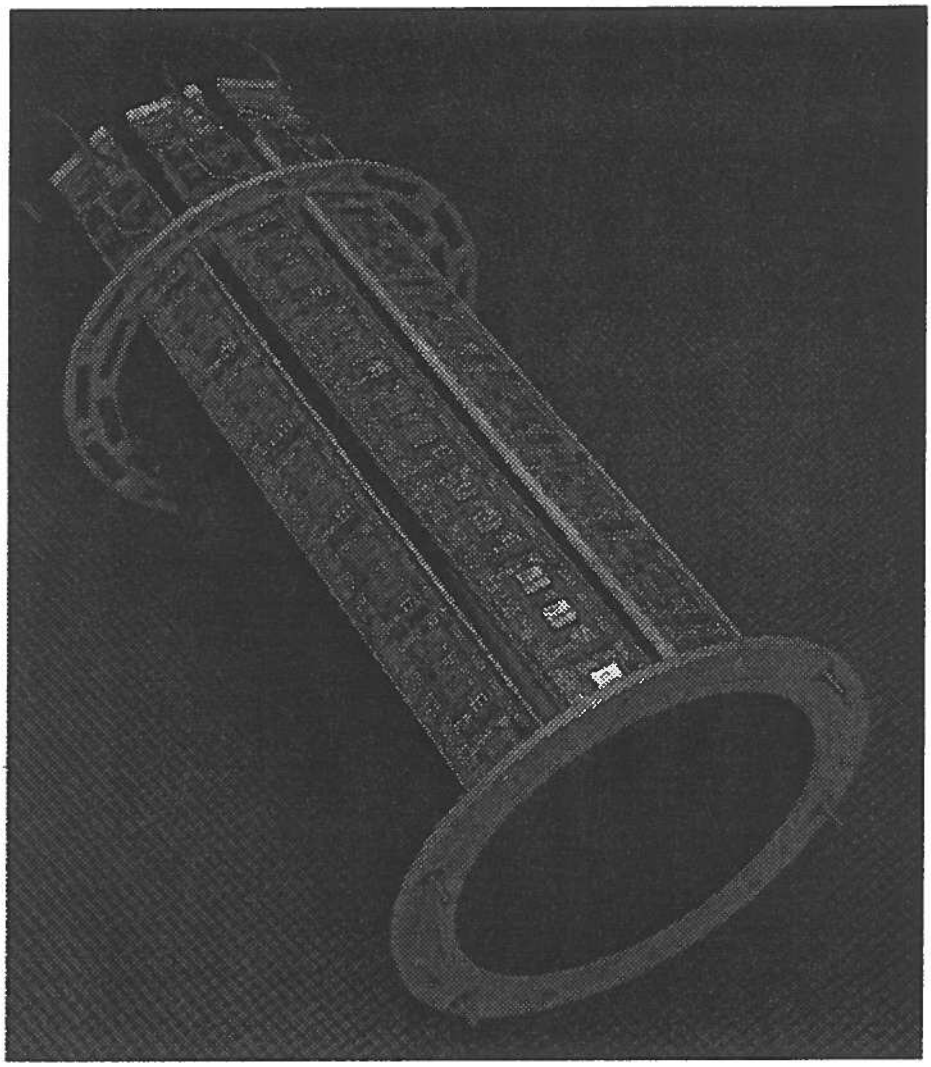

Fig. 12. *The carbon fiber support with three inner slabs (short type) already mounted; the two vetronite flanges are clearly visible together with the power supply twin cables. Flat cables for signals and controls are not shown.*

Both flanges are glued to the carbon fiber cylinder using araldit to form a reel shape support which all *slabs* have been hung on to.

The whole cylinder is then covered with a vetronite sheet (0.1 mm thick) whose external face is covered with a thin layer of carbon paint in order to protect it from light and dust and to provide a shield from external electromagnetic noise (both internal and external cylinder are grounded).

The total weight is 2.2 Kg excluding read-out cables, for a 90 degrees estimated radiation lenght around 3.5% X_0 [11]

[11] Detector thickness is not uniform at all and depends both on θ and ϕ; thickness ranges between 2.0 and 4.5% X_0 giving the smeared value quoted in the text.

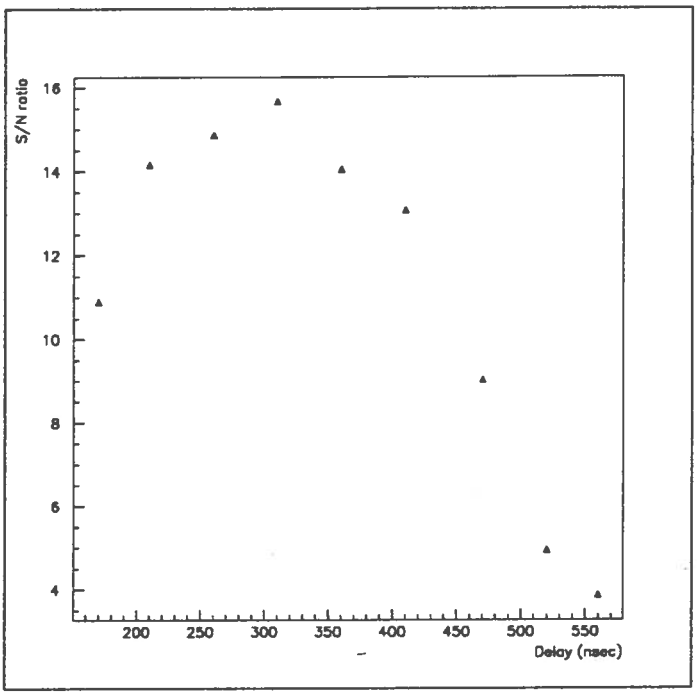

Fig. 13. *Signal / Noise ratio measured as a function of Track & Hold delay with respect to particle crossing time.*

As we said in section 3, power dissipated by one single PCB is above 5 W, giving a total absorption of about 130 W. Silicon detector performance is badly spoiled at high temperature, so a suitable cooling system must be provided. In order to minimize non active material inside detector acceptance, we decided not to use a refrigerating liquid. Gas cooling is enough to achieve a working temperature around 35 degrees Celsius using a gas flow about 3.5 l/s with an input temperature around 15 degrees. In principle nitrogen would have been the best choice but practical and cost concerns have led us to use a clean and dry air flow.

5 Cosmic rays and test beam results

The SPD has been tested both using cosmic rays and a 5 GeV/c π^- beam in two different periods at the CERN Hall East (a prototype with just two crystals during november 1994 and 50% of the whole detector in october/november 1995).

The first beam test was devoted to study detector response to minimum ionizing particles and to measure its signal/noise ratio; to have a deeper insight into detector performance, we decided to use an analog read-out based on a

digital scope together with the digital read-out [12].

In this way we could read out about 1000 ICAR16 waveforms triggered by real minimum ionizing particles, which have been used to study detector response. An example of these waveforms is shown in Figure 10 where the signal due to a charged particle traversing the crystal at 90 degrees is clearly visible together with 15 small spikes due to other empty channels .

Figure 13 shows the S/N ratio as a function of Track & Hold delay, being $\Delta t = 0$ at the particle crossing time; the best performance is achieved with $\Delta t = 300\ ns$ where S/N $\simeq 15$ [13].

The second beam test was meant to measure detector efficiency, position resolution and noise in operating condition similar to those we will have in E-835 experiment, using a statistically significant sample of channels (50% of the whole detector, 2304 channels). We set a tower of 12 slabs on the T10 test beam, using 3 "finger" scintillators as a trigger. About 10^6 minimum ionizing particle events have been recorded, with different thresholds and bias voltage in order to optimize these parameters and find the best operating conditions. To set the proper thresholds we first performed a scan, reading out 500 times the whole detector with different thresholds starting from values well below the ICAR16 DC output level and going well above; in this way a curve similar to the one shown in Figure 14 is obtained for each channel; by fitting this curve with a complementary error function, we can measure both the average DC value and noise standard deviation with good accuracy.

Figure 15 shows the same plot as obtained with the pion beam on; in this case the fit is done with a function that is the sum of a complementary error function and an integrated Landau distribution, from which we got the measurement of the Signal/Noise ratio shown in Figure 13. When thresholds are set 4 or 5 σ above ICAR16 DC values, 98 % of the channels work fine; remaining 2% of the channels is still noisy because of two main reasons:

1) Some ICAR16 have non uniform output DC value; for we have one single threshold per ICAR16, sometimes it is not possible to take this thresholds above each channel without loosing efficiency on the others [14].

---

[12] On each slab the output signal of one single ICAR16 (out of 12) is also connected to an analog driver and delivered to the external read-out electronics for test and monitoring.

[13] The Track & Hold delay dependence of the S/N ratio is quite obvious but it is very critical in our experiment; being set in a DC collider we have no time information about the beam crossing, so we have to use the first level trigger to strobe the detector; the result shown in Figure 13 is very important because 300 ns is just what the trigger system needs to process the signals and strobe good events.

[14] We could not afford to reject all chips with non uniform DC output.

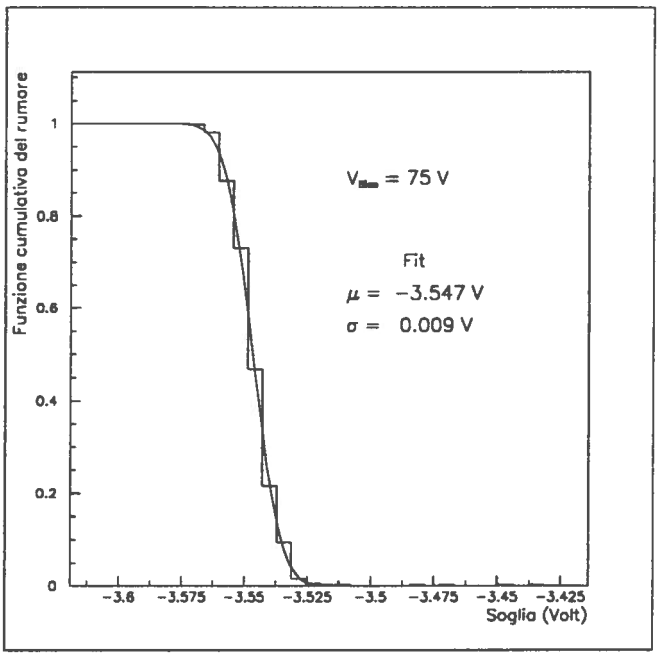

Fig. 14. *This plot shows the result of a threshold scan performed with beam off (pure noise); the vertical axis is the number of times the channel is ON while the orizontal axis is the threshold measured in V. The curve is a complementary error function while the numbers shown are the fit results.*

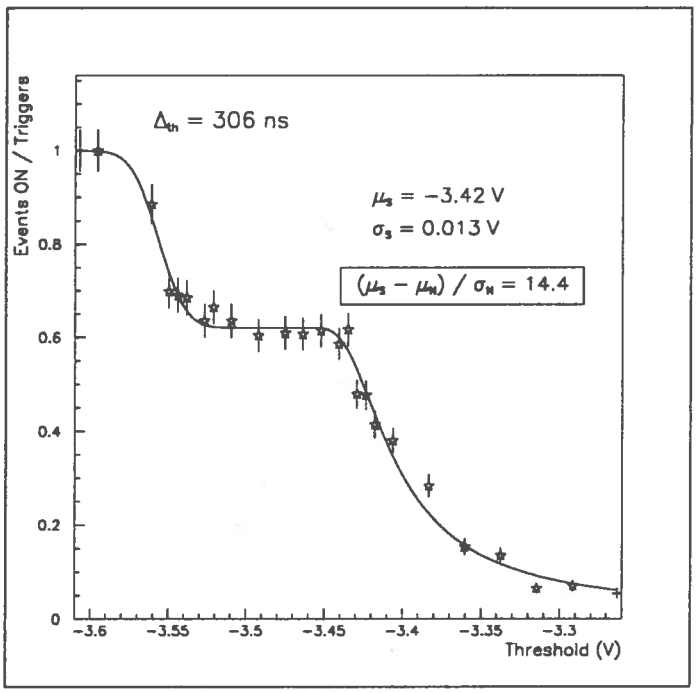

Fig. 15. *This plot shows the result of a threshold scan performed with beam on; the vertical axis is the number of times the channel is ON while the orizontal axis is the threshold in V. The curve is a complementary error function to fit the noise contribution as in Figure 14 plus an integrated Landau distribution to include the contribution due to minimum ionizing particles.*

2) Some channels are always ON because of large diode current.

Being all crystals set on two layers, the overall effect of these noisy channels on real efficiency is small.

Figure 16 shows the fitted residual of beam tracks hitting one slab at an angle of 30 degreees; resolution is what is expected with two layers of 2.9 mm wide pads (the number of two hits clusters is around 1% and gives no important contribution to geometrical resolution).

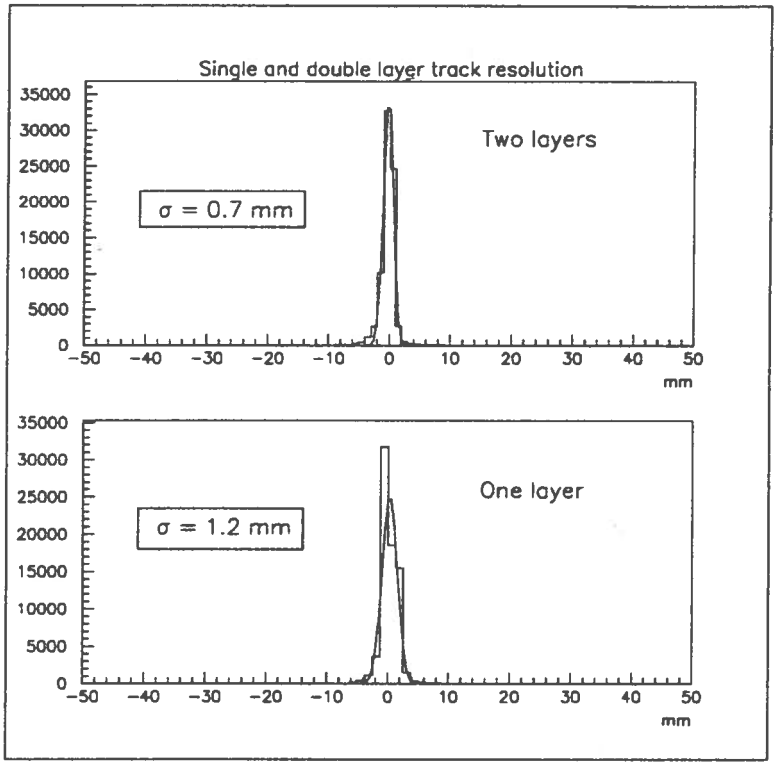

Fig. 16. Track resolution for 30 degrees tracks hitting both layers of one slab; upper plot is the resolution obtained using the information of both hits in the two staggered layers while lower plot shows the single pad resolution; the number of tracks which are associated to a cluster of hits in the same layer is negligible (around 1%) and gives no contribution to the resolution.

6 Acknowledgements

Many people have helped us to complete this project successfully.

The constant advice and encouragement by Prof. A. Santroni and Dr. M. Macrì were precious.

We are also deeply in debt with I.N.F.N. technicians G. Barisone, S. Minutoli, M. Negri, P. Poggi who have contributed on detector design and have built it. We are also glad to acknowledge the work of G. Massari, M. Olcese, P. Pozzo on mechanical engineering and drawings and all people of the I.N.F.N. Mechanical Department.

The work of people of I.N.F.N.'s Electronics Department A. Bevilacqua and F. Siccardi on electronics design and testing has been precious.

We also thank G. Darbo and L. Rossi (I.N.F.N. Genova) for their useful advice.